PRAMANA
— journal of
physics

Vol. 57, Nos 5 & 6
Nov. & Dec. 2001
pp. 1129–1138

Spatiotemporal solitons in quadratic nonlinear media

FRANK W WISE
Department of Applied Physics, 212 Clark Hall, Cornell University, Ithaca, New York 14853, USA

Abstract. Recent developments in the study of optical spatiotemporal solitons are reviewed.

Keywords. Solitons; nonlinear pulse propagation; nonlinear optics; cascade nonlinearity; femtosecond pulses; ultrafast phenomena.

PACS Nos 42.65.Tg; 045.45.Yv; 42.65.Ky; 42.65.Re; 42.65.Sf

1. Introduction

Optical solitons are localized electromagnetic waves that propagate stably in nonlinear media with group-velocity dispersion (GVD) and/or diffraction. Temporal solitons in single-mode optical fibers are the prototypical optical solitons; these were predicted theoretically in 1973 [1] and first observed experimentally in 1980 [2]. Extensive research since then has led to the current development of telecommunication systems based on solitons [3].

Compared to the work on temporal solitons, progress in the area of multidimensional (spatial or spatiotemporal) optical solitons has been much slower. Like temporal solitons, in cubic $(\chi^{(3)})$ nonlinear media these waves are also governed by nonlinear Schrödinger equations (NLSE). It has long been understood that self-focussing as a result of the (cubic) Kerr nonlinearity could compensate for the spreading of a beam due to diffraction, but the resulting balance is unstable in > 1 dimension [4]; the beam tends to diffract, collapse, or disintegrate into multiple filaments. However, processes not included in the NLSE may stabilize self-trapped beams. Spatial solitons were first produced in liquid CS_2, where an interference grating was employed to stabilize the solitons [5], and light filaments were observed [6] in resonant propagation through an atomic vapor, where the nonlinearity is saturable. One-dimensional (1D) spatial solitons of the NLSE were generated in a glass waveguide in 1990 [7].

Studies of spatial solitons began to make rapid progress in the1990s, when two new types of soliton-supporting nonlinear-optical interactions were identified. Segev *et al* [8] predicted that the photorefractive effect in electro-optic materials could be used to create a saturable nonlinear index of refraction that would support soliton formation. Photorefractive solitons were observed soon afterwards [9], and since then a variety of such solitons has been reported in 1D and 2D [10]. At nearly the same time, there was a resurgence of interest in an effective cubic nonlinearity that is produced by the interaction of two or three waves in quadratic $(\chi^{(2)})$ nonlinear media [11]. The renewed interest was based

on the recognition that large, effective third-order nonlinearities of controllable sign can be produced. An additional property is that the effective nonlinearity saturates, so self-focussing collapse can be avoided in quadratic media [12]. Thus, quadratic media possess the properties required for multidimensional soliton formation [13], and numerous theoretical treatments of solitons in quadratic media appeared in the early 1990s [14]. Torruellas *et al* first observed stationary spatial solitons [15], and Di Trapani and co-workers produced temporal solitons in quadratic media [16]. Very recently, Di Trapani *et al* reported the observation of vortex solitons in quadratic media [17].

Photorefractive and quadratic solitons are profoundly different from solitons in one-dimensional Kerr media. As an illustration of the differences, in quadratic media the soliton actually consists of two fields at different frequencies, coupled and mutually trapped by the nonlinear interaction. Because they are solutions of non-integrable systems, solitons in quadratic and photorefractive media can participate in a variety of phenomena not available to temporal solitons in optical fibers. For example, soliton fission, annihilation, and stable orbiting in three dimensions are all possible.

One of the major goals in the field of soliton physics is the production of light fields that are localized in all three dimensions of space as well as time, which we will refer to as 3D spatiotemporal solitons (STS). These result from the simultaneous balance of diffraction and GVD by self-focussing and nonlinear phase-modulation, respectively (figure 1). The possibility of such pulses in multiple dimensions was considered by Silberberg [18], who is generally credited with coining the term '*light bullets*' to describe them. It is well-known that 3D STS are unstable against collapse in cubic nonlinear media [19], but solutions may be stabilized if the nonlinearity is saturable, or if additional nonlinear processes such as multiphoton ionization exist to arrest the collapse favored by self-focussing. Their scientific importance has motivated a number of theoretical studies of STS in quadratic media [20–24].

The first experimental studies of optical STS were reported last year [25–27]. This paper will briefly review and summarize the key aspects of those experiments.

2. Pulse propagation in quadratic media

Within the slowly-varying envelope approximation, the equations that govern the interaction of fundamental harmonic (FH) and second harmonic (SH) electric fields (E_1 and E_2, respectively) that propagate in the z direction (and assumed constant in the x direction) in a medium with quadratic and cubic nonlinearity are

$$\begin{aligned}
&\left(\frac{\partial}{\partial z}+\frac{iL_{NL}}{4L_{DS1}}\frac{\partial^2}{\partial t^2}+\frac{iL_{NL}}{4L_{DF1}}\frac{\partial^2}{\partial y^2}\right)E_1\\
&\qquad=iE_1^*E_2\mathrm{e}^{i\Delta kz}+i2\pi(n_2I_0)\frac{L_{NL}}{\lambda}\left(|E_1|^2+\frac{2}{3}|E_2|^2\right)E_1\\
&\left(\frac{\partial}{\partial z}+\frac{L_{NL}}{L_{GVM}}\frac{\partial}{\partial t}+\frac{iL_{NL}}{4L_{DS2}}\frac{\partial^2}{\partial t^2}+\frac{iL_{NL}}{4L_{DF2}}\frac{\partial^2}{\partial y^2}\right)E_2\\
&\qquad=iE_1E_1\mathrm{e}^{i\Delta kz}+i4\pi(n_2I_0)\frac{L_{NL}}{\lambda}\left(\frac{2}{3}|E_1|^2+|E_2|^2\right)E_2.
\end{aligned}\tag{1}$$

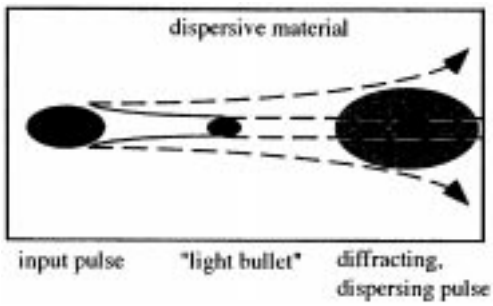

Figure 1. Illustration of ordinary propagation of a short pulse in a nonlinear, dispersive medium, along with the formation of STS.

E_1 and E_2 are in units of the initial peak FH field E_0 (related to the initial peak FH intensity by $I_0 = \sqrt{\varepsilon/\mu}|E_0|^2/2$), n_2 is the Kerr nonlinear index, and $\Delta k = k_{2\omega} - 2k_\omega$ is the wave-vector mismatch between fundamental and harmonic fields. The diffraction, dispersion, and nonlinear lengths characterizing the pulse propagation are $L_{DF} = k\omega_0^2/2$, $L_{DS} = 0.322\tau_0^2/|\beta^{(2)}|$, and $L_{NL} = n\lambda/\pi\chi^{(2)}E_0$, respectively, where λ is the FH wavelength. Time t is measured in units of the initial pulse duration τ_0, and positions z and y are measured in units of L_{NL} and the y-dimension beam waist ω_0, respectively. $\beta^{(2)}$ is the GVD, which will have contributions from both material dispersion and angular dispersion. The characteristic length over which the FH and SH pulses walk away from each other in time as a consequence of the group-velocity mismatch (GVM) is $L_{\mathrm{GVM}} = c\tau_0/(n_{1g} - n_{2g})$, with n_{1g} and n_{2g} the group indices at the FH and SH frequencies, respectively.

The effective cubic nonlinearity in quadratic media results from the cascading of $\chi^{(2)}(2\omega;\omega;\omega)$ (conversion) and $\chi^{(2)}(\omega;2\omega;-\omega)$ (back-conversion) processes in phase-mismatched second harmonic generation (SHG). The process of conversion and back-conversion generates a nonlinear phase shift $\Delta\Phi^{NL}$ at the FH frequency. For large phase mismatch or low intensity, the nonlinear phase shift can be approximated as $\Delta\Phi_{NL} \approx -\Gamma^2L^2/\Delta kL$, where $\Gamma = d_{\mathrm{eff}}\omega|E_0|/c\sqrt{n_\omega n_{2\omega}}$ [11]. Depending on the sign of of the phase-mismatch ΔkL, the phase shift can be either self-focusing ($\Delta kL < 0, \Delta\Phi_{NL} > 0$) or self-defocusing ($\Delta kL > 0, \Delta\Phi_{NL} < 0$).

Pulse propagation is modeled by numerically solving the coupled wave equations, using a symmetric split-step beam-propagation method: a Runge-Kutta algorithm solves the nonlinear propagation step in the time domain, and the dispersive and diffractive propagation steps are solved in the frequency domain. Some results of the numerical solutions will be compared with experimental data below.

3. Solitons in one transverse spatial dimension and time

Once the saturable nonlinearity is identified, the greatest experimental challenge to the generation of STS is the requirement of anomalous GVD at both fundamental and second-harmonic wavelengths [23]. The magnitude of the anomalous GVD should be large enough to produce a characteristic dispersion length (L_{DS}) commensurate with the dimensions of available quadratic nonlinear crystals. For practical purposes, this means $L_{DS} \sim 5$ mm,

which implies GVD ∼10 times larger than that of typical transparent materials. The focusing, pulse energy, and phase mismatch can be conveniently adjusted to produce L_{DF} and L_{NL} in this range. We create an environment with such strong anomalous GVD by use of a trick that is common in the femtosecond-optics community: angular dispersion of the input pulse using a diffraction grating produces large and anomalous GVD [28]. Diffraction from a grating can also be used to match the group velocities of the FH and SH pulses; then each wavelength in the pulse spectrum propagates at its phase-matching angle. However, GVD and GVM cannot be chosen independently. A limitation of this approach is that the use of the diffraction grating to disperse wavelengths in one direction precludes the production of STS confined in both transverse dimensions. The experimental apparatus implements the situation shown in figure 2. A Ti-sapphire regenerative amplifier produces pulses of duration 120 fs and energy up to 1 mJ at a wavelength of ∼ 800 nm. The pulses diffract off a grating and pass though a telescope and a cylindrical lens prior to incidence on the SHG crystal (lithium iodate or barium borate, cut for type-I interaction). The grating disperses the spectrum in the horizontal transverse (x) direction, and the cylindrical lens focuses the beam in the y direction. The beam waist in the unfocused (x) direction is 3-4 mm, so diffraction is negligible in that direction. Following the crystal, the optics are repeated in reverse order to compensate the dispersion imposed by the grating and to collimate the beam. To image the beam at the exit face of the crystal, the second cylindrical lens is removed, and the beam is imaged with a spherical lens following the second grating. Details of the experimental arrangement can be found in [26].

In general, the fundamental and harmonic fields propagating in a quadratic medium will have different group velocities, and the resulting GVM will impact the properties of STS. Intuitively, if the two fields have distinct velocities, they will move apart from each other in linear propagation. This hinders the formation of STS, in which the fields mutually trap each other. Given this concern, we first performed experiments with nearly equal group velocities at fundamental and harmonic frequencies. In $LiIO_3$, zero GVM can be obtained simultaneously with $L_{DS} \approx 3$ mm, so $LiIO_3$ was chosen for experiments with zero GVM. To investigate the effects of GVM on STS formation, a series of experiments was performed under conditions of large GVM between FH and SH fields. These experiments employed barium metaborate (BBO) as the quadratic nonlinear medium.

First we briefly summarize the results of experiments aimed at producing STS under conditions of nearly-zero GVM between FH and SH fields. With the $LiIO_3$ crystal oriented to produce self-focusing cascade phase shifts, the pulse duration and beam profile at the output face of the crystal vary with the incident intensity I_0. For $I_0 < 1$ GW/cm^2, the

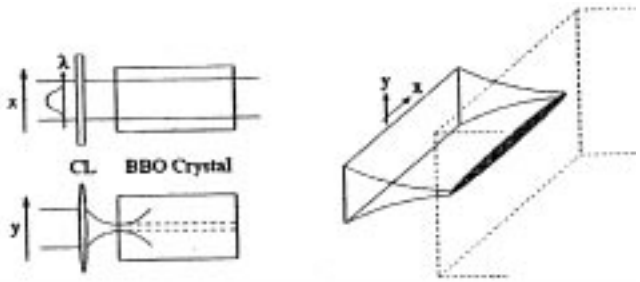

Figure 2. Schematic of the experimental arrangement to study 2D STS.

pulse (beam) broadens in time (space) owing to dispersion and diffraction. At higher intensities space-time focusing is observed, which is already significant consdering that it is not stable in cubic nonlinear media. With $I_0 \sim 10$ GW/cm^2 the output pulse essentially matches the input, which is the first evidence of soliton formation. The pulses overcome diffraction in one transverse spatial dimension, as well as GVD, to reach constant beam size and pulse duration; we call these 2D STS. At higher intensities (up to $I_0 \sim 80$ GW/cm^2), solitons still form but their propagation is periodic. The pulse (beam) compresses and expands by a factor as large as 3, so the intensity varies by nearly a factor of 10.

In the absence of GVM, time and the transverse spatial coordinates are formally equivalent in the coupled wave equations. However, quadratic solitons consist of two fields at distinct frequencies, so GVM is a general feature of the problem and it is essential to determine its consequences. In the presence of GVM, the problem becomes anisotropic in the transverse dimensions, so the spatiotemporal nature of the problem is emphasized. As a consequence, for example, we do not expect the same behavior from 2D STS and 2-dimensional spatial solitons because time is not equivalent to a transverse spatial dimension. The GVD and birefringence of BBO allow one to perform experiments at 800 nm with the relatively large value $L_{DS}/L_{GVM} \sim 3$; i.e. the two pulses would move apart by 3 times the pulse duration in one dispersion length. In contrast to $LiIO_3$, BBO has small nonlinear index of refraction and negligible 2-photon absorption around 400 nm. Considering these issues, Liu *et al* focused their attention primarily on the generation of STS with large GVM.

Numerical solutions of the coupled wave equations show that STS should form despite the presence of GVM, as long as the magnitude of the phase-mismatch is chosen to be sufficiently large. An example is shown in figure 3. With the phase mismatch set near the optimum value for STS formation as determined by the numerical simulations, stable

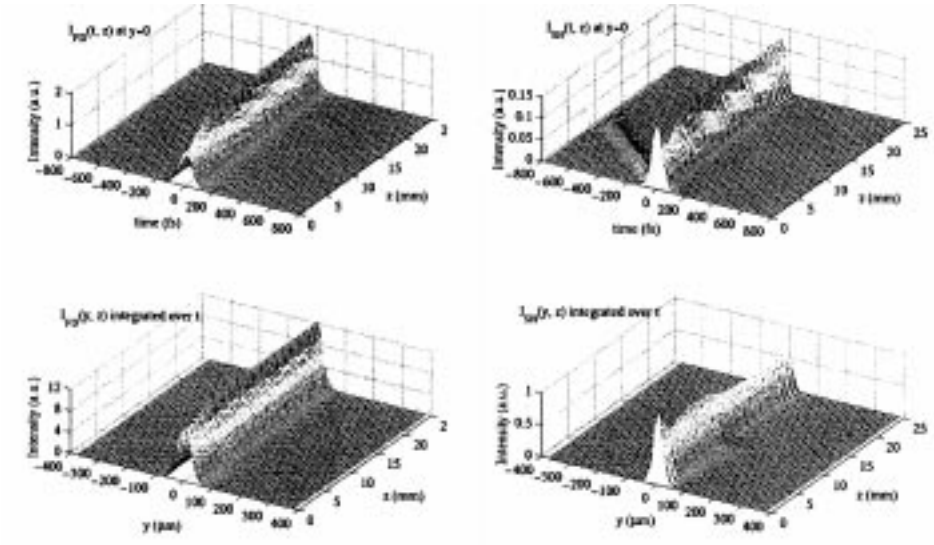

Figure 3. Numerical simulation of STS in the presence of large GVM. Temporal and spatial evolution of fundamental and second-harmonic fields are shown.

pulse duration and beam profile are indeed observed experimentally over 5 characteristic lengths. Typical experimental data are shown in figure 4. The experimental conditions (input intensity and phase mismatch) required to produce STS agree reasonably well with the numerical solutions.

From the measurements made after propagation $\sim$3 and $\sim$5 characteristic lengths and the numerical simulations, we conclude that STS are formed in BBO for parameters in the vicinity of $\Delta kL \approx -44\pi$ and $I_0 \approx 8$ GW/cm^2. Because the input pulse is reasonably close to the STS solution, stable mutual trapping occurs in a short propagation distance ($\sim$1 characteristic length) and the pulse sheds minimal energy as it evolves. After propagation through the BBO crystal, we find that the SH energy is $\sim$2-4% of the input pulse energy, as expected given the large phase mismatch. The total energy is conserved to within a few percent. The absence of 2-photon absorption at 400 nm and the small Kerr nonlinearity in BBO make these experiments a nearly ideal realization of the theoretical model (eq. (1)). The fact that STS can still be formed despite the large difference in group velocities is a measure of the strength of the nonlinear coupling.

At intensities just above the threshold intensity for STS formation, STS still occur but they evolve periodically. In some sense, these STS are analogous to the solitons of the nonlinear Schrödinger equation with $N > 1$. However, it is important to keep in mind that STS occur over continuous range of energies in quadratic media, in contrast to the discrete soliton energies in cubic nonlinear media.

An extensive series of measurements of pulse propagation with varying input intensity (I_0) and phase mismatch (ΔkL) allowed Liu *et al* [26] to establish the range of parameters over which STS form. At low intensities or large phase mismatch, dispersive and diffractive broadening is observed. STS form in a narrow range of coordinates in the $I_0 - \Delta kL$ plane. This region is bounded below by the need for adequate nonlinear phase shift: larger phase mismatch can be tolerated at higher intensities. STS are not observed for $\Delta kL < -100\pi$, at any intensity; although adequate phase shift can be generated, saturation is inadequate to stabilize the STS under these conditions. STS also cannot be formed if the phase mismatch is too close to zero. Near phase-matching, the FH and SH pulses may move apart in time before mutual trapping can take place. Increasing $\Delta\Phi_{NL}$ from the values that produce STS, either by decreasing $|\Delta kL|$ or by increasing I_0, causes the 2D STS in the form of a stripe to break up into a series of filaments. This will be discussed below. Finally, at the highest intensities, the unavoidable cubic nonlinearity of BBO causes self-focusing collapse, which is evidenced as severe beam distortions and the generation of 'white-light' continuum.

4. Transverse instability of STS: Toward light bullets

As mentioned above, one of the limitations to the formation of STS is transverse instability (TI). Starting from conditions that produce STS, if the input intensity is increased or the phase mismatch is decreased, the 2D STS breaks up into a set of filaments, as illustrated in the spatial profile measured at 12 GW/cm^2 (figure 4). The dependence of the filaments on input intensity and phase mismatch are consistent with calculations, which demonstrates that TI is the origin of the breakup [27]. The numerical calculations also show that the filaments produced through TI will be 3D STS if the environment has the correct group-velocity dispersion to support STS.

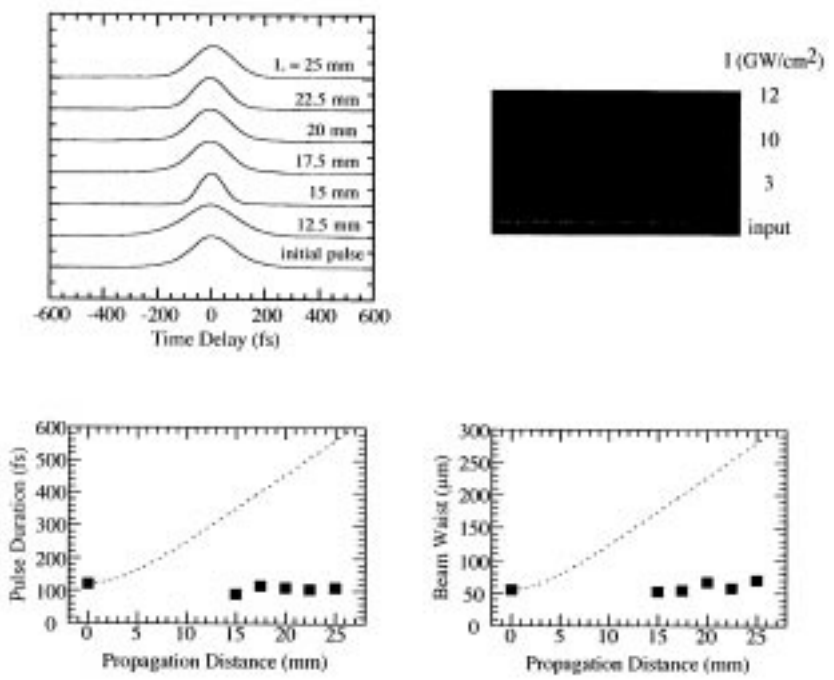

Figure 4. Experimental evidences of STS under conditions of large GVM. The top two panels show raw data for pulse duration and beam profile. The pulse duration is measured after different distances under conditions of fixed intensity, while the beam profiles are shown for a single propagation distance and varying intensity. The bottom two panels show pulse duration and beam waist obtained from raw data exemplified by the top two panels and plotted versus distance. The dashed lines in the bottom panels indicate the evolution in linear propagation.

In the experiments of Liu *et al*, the beam fragments into filaments that are initially elliptical in shape, with an aspect ratio of ∼4:3. Measurements of individual filamets show that the pulse duration is ∼100 fs, the same as for the 2D STS. These filaments quickly evolve to the circular cross section expected for 3D STS, but eventually broaden in time and space as a consequence of our use of the diffraction grating to produce GVD. Thus, true 3D STS are not observed, but the experiments demonstrate that production of 3D STS through TI of the 2D STS will occur if the GVD is not produced using diffraction gratings.

The transverse instability is closely connected to the periodic evolution of STS in quadratic media. In cubic nonlinear media, the spatial frequency at which the TI gain is maximum (which is the observed spatial frequency in practice), increases slowly with input intensity, $\Omega_{\max} \sim I_0^{1/4}$ – this intensity-dependence is viewed as the hallmark signature of TI. Liu *et al* found that the filament spatial frequency varies much more rapidly than this for STS in quadratic media. Analytic and numerical calculations show that the intensity-dependence can be understood using the same $I^{1/4}$ dependence, as long as the appropriate value of I is used. It is important to recall that the evolution of STS in quadratic media is generally periodic. TI is most likely to occur at the points of highest intensity,

simply because that is where the TI gain will be maximum. Once one realizes that the maximum intensity achieved by the 2D STS is the appropriate value, the TI of STS can be understood in terms of an effective cubic nonlinearity. It is interesting to note that only the fully-confined light bullet is truly stable; all lower-dimensional solitons are susceptible to TI.

5. Spatiotemporal solitons through non-collinear second-harmonic generation

Finally, Liu *et al* recently showed that 2D STS can be generated through non-collinear SHG [29]. The main idea for this experiment was proposed by Drummond *et al* [30]. Non-collinear input beams that are not solitons interact, and an output 2D STS appears at the bisector of the angle between the inputs (figure 5). This experiment helps us understand the detailed mechanisms by which the fundamental fields self-focus while the fundamental and harmonic fields couple and trap each other. Since the output STS only appears

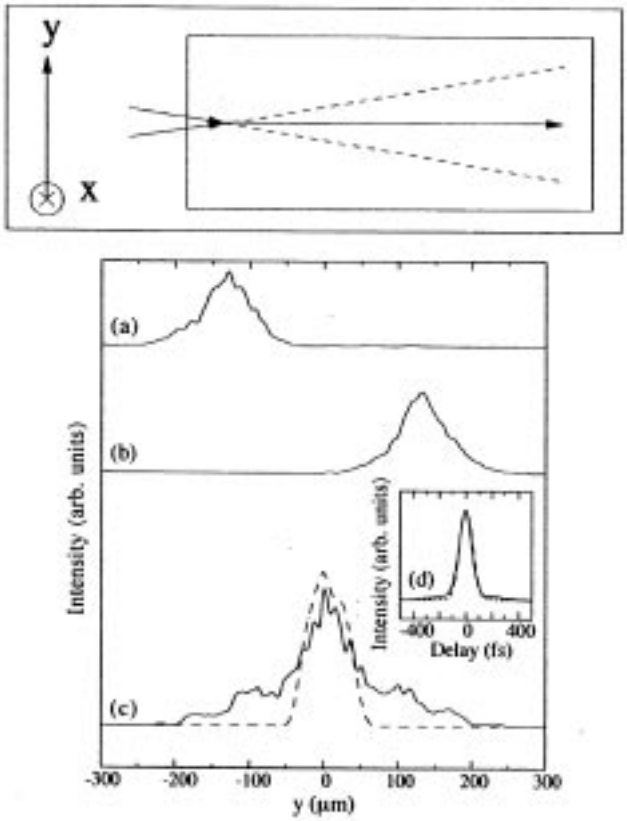

Figure 5. The top panel illustrates noncollinear generation of STS and bottom panel presents experimental results. STS produced by one input beam are shown in (a) and (b), and STS produced with both input beams present are shown in (c). The inset shows the temporal profiles of the input pulse and the STS generated by noncollinear SHG.

when both the inputs are present, this mechanism could be the basis for an all-optical AND gate. Compared to interacting solitons, this type of interaction will be much less phase-sensitive, which should be an advantage in applications. Information-processing systems based on spatiotemporal solitons could have bandwidths of many terahertz, and this motivates further investigation of soliton production and interactions in this context.

6. Conclusions and future directions

The initial demonstrations of STS by Liu and co-workers makes it possible to plan studies of a number of intriguiging aspects of STS. Interactions among STS are of great scientific interest, and will be the basis of soliton logic. Collisions in saturable nonlinear media exhibit a greater variety of phenomena than those in Kerr media; the coupled wave equations are not integrable, so interactions are accompanied by radiation, and soliton number is not conserved. Thus, annihilation, fission, and fusion of STS are all possible. We hope to investigate these phenomena in the near future.

Of course, there is still great interest in the direct generation of 3D STS, the true light bullets. By the use of Bragg gratings or more general periodic structures it may be possible to create an environment that will support 3D STS, and this is another direction that we hope to pursue in the near future.

Acknowledgements

The author thanks Xiang Liu, LieJia Qian, and Kale Beckwitt, whose efforts produced the results described here, and acknowledges stimulating discussions with B Malomed, L Torner, J P Torres, and P Drummond. This work was supported by the National Science Foundation and the National Institutes of Health, USA.

References

[1] A Hasegawa and F Tappert, *Appl. Phys. Lett.* **23**, 142 (1973)
[2] L F Mollenauer, R H Stolen and J P Gordon, *Phys. Rev. Lett.* **45**, 1095 (1980)
[3] See, for example, G P Agrawal, *Fiber-optics communication systems* (Wiley, New York, 1992)
[4] V E Zakharov and A M Rubenchik, *Sov. Phys. JETP* **38**, 494 (1974)
[5] A Barthelemy, S Maneuf and C Froehly, *Opt. Commun.* **55**, 201 (1985)
[6] J E Bjorkholm and A Ashkin, *Phys. Rev. Lett.* **32**, 129 (1974)
[7] J S Aitchison, A M Wiener, Y Silberberg, M K Oliver, J L Jackel, D E Leaird, E M Vogel and P W E Smith, *Opt. Lett.* **15**, 471 (1990)
[8] M Segev, B Crosignani, A Yariv and B Fischer, *Phys. Rev. Lett.* **68**, 923 (1992)
[9] G Duree, J L Schultz, G Salamo, M Segev, A Yariv, B Crosignani, P DiPorto, E Sharp and R Neurgaonkar, *Phys. Rev. Lett.* **71**, 533 (1993)
[10] M Segev, *Opt. Quantum Electron.* **30**, 503 (1998)
[11] J-M R Thomas and J-P E Taran, *Opt. Commun.* **4**, 329 (1972)
N R Belashenkov, S V Gagarskii and M V Inochkin, *Opt. Spectrosc.* **66**, 806 (1989)
H J Bakker, P C M Planken, L Kuipers and A Lagendijk, *Phy. Rev.* **A42**, 4085 (1990)

R DeSalvo, D J Hagan, M Shiek-Bahae, G Stegeman, E W Van Stryland and H Vanherzeele, *Opt. Lett.* **17**, 28 (1992)
[12] A A Kanashov and A M Rubenchik, *Physica* **D4**, 122 (1981)
[13] Y N Karamzin and A P Sukhorukov, *Sov. Phys. JETP* **41**, 414 (1976)
[14] For example: C R Menyuk, R Schiek and L Torner, *J. Opt. Soc. Am.* **B11**, 2434 (1994)
A V Buryak and Y S Kivshar, *Opt. Lett.* **19**, 1612 (1994)
L Torner, C R Menyuk and G I Stegeman, *Opt. Lett.* **19**, 1615 (1994)
S K Turitsyn, *JETP Lett.* **61**, 469 (1995)
L Berge, V K Mezentsev, J J Rasmussen and J Wyller, *Phys. Rev.* **A52**, R28 (1995)
[15] W E Torruellas, Z Wang, D J Hagan, E W Van Stryland, G Stegeman, L Torner and C R Menyuk, *Phys. Rev. Lett.* **74**, 5036 (1995)
[16] P Di Trapani, D Caironi, G Valiulis, A Dubietis, R Danielius and A Piskarskas, *Phys. Rev. Lett.* **81**, 570 (1998)
[17] P Di Trapani, W Chinaglia, S Minardi, A Piskarskas and G Valiulis, *Phys. Rev. Lett.* **84**, 3843 (2000)
[18] Y Silberberg, *Opt. Lett.* **15**, 1282 (1990)
[19] E A Kuznetsov, A M Rubenchik and V E Zakharov, *Phys. Rep.* **142**, 105 (1986)
J J Rasmussen and K Rypdal, *Phys. Scr.* **33**, 481 (1986)
[20] Y N Karamzin and A P Sukhorukov, *Sov. Phys. JETP* **41**, 414 (1976)
[21] H He, M J Werner and P Drummond, *Phys. Rev.* **E54**, 896 (1996)
[22] D Mihalache, D Mazilu, B A Malomed and L Torner, *Opt. Commun.* **152**, 365 (1998)
[23] B A Malomed, P Drummond, H He, a Berntson, D Anderson and M Lisak, *Phys. Rev.* **E56**, 4725 (1997)
[24] D Mihalache, D Mazilu, L-C Crasovan, L Torner, B A Malomed and F Lederer, *Phys. Rev.* **E62**, 7340 (2000)
[25] X Liu, L J Qian and F W Wise, *Phys. Rev. Lett.* **82**, 4631 (1999)
[26] X Liu, K Beckwitt and F W Wise, *Phys. Rev.* **E62**, 1328 (2000)
[27] X Liu, K Beckwitt and F W Wise, *Phys. Rev. Lett.* **85**, 1871 (2000)
[28] O E Martinez, *IEEE J. Quantum Electron.* **25**, 2464 (1989)
[29] X Liu, K Beckwitt and F W Wise, *Phys. Rev. E (Rapid Communications)* **61**, R4722 (2000)
[30] P Drummond, K V Kheruntsyan and H He, *J. Opt. B: Quantum semiclassical Opt.* **1**, 387 (1999)